High-refractive-index TiO_2-nanoparticle-loaded encapsulants for light-emitting diodes

Frank W. Mont,[1] Jong Kyu Kim,[1] Martin F. Schubert,[1] E. Fred Schubert,[1,a)] and Richard W. Siegel[2]
[1]*Future Chips Constellation, Department of Electrical, Computer, and Systems Engineering, Rensselaer Polytechnic Institute, Troy, New York 12180, USA*
[2]*Department of Materials Science & Engineering and Rensselaer Nanotechnology Center, Rensselaer Polytechnic Institute, Troy, New York 12180, USA*

(Received 10 September 2007; accepted 5 February 2008; published online 25 April 2008)

A high-refractive-index (high-n) encapsulant is highly desirable because it can result in enhancement of light-extraction efficiency from high-n semiconductor light-emitting diode (LED) chips. A uniform dispersion of TiO_2 nanoparticles in epoxy for LED encapsulation is demonstrated for surfactant-coated TiO_2 nanoparticles by drying, mixing with a solvent, refluxing, centrifuging, and mixing with epoxy. The refractive index of surfactant-coated TiO_2-nanoparticle-loaded epoxy is 1.67 at 500 nm, significantly higher than that of conventional epoxy ($n=1.53$). Theoretical analysis of optical scattering in nanoparticle-loaded encapsulants reveals that the diameter of nanoparticles and the volume loading fraction of nanoparticles are of critical importance for optical scattering. Quasispecular transparency of the encapsulant film can be achieved if the thickness of the film is kept below the optical scattering length. A graded-refractive-index multilayer encapsulation structure with the thickness of each layer being less than the mean optical scattering length is proposed in order to reduce optical losses from scattering and Fresnel reflection. Furthermore, three-dimensional optical ray-tracing simulations demonstrate that encapsulants with an optimized scattering coefficient, k_s, benefit from optical scattering by extracting deterministic trapped modes. Theoretical light-extraction enhancements larger than 50% are found when comparing scattering-free to scattering encapsulation materials. © *2008 American Institute of Physics*. [DOI: 10.1063/1.2903484]

I. INTRODUCTION

One of the fundamental limitations in the light-extraction efficiency of light-emitting diodes (LEDs) is the occurrence of trapped light within high-refractive-index (high-n) semiconductors such as III-V phosphides, arsenides, and nitrides. Based on Snell's law, the angle of the light-escape cone for the semiconductor-air interface is very small due to the high-refractive-index contrast. For example, the escape-cone angle for unencapsulated AlGaInP ($n_{\mathrm{AlGaInP}}=3.35$) is only ~17°, resulting in light-extraction efficiencies of only a few percent. The light outside the escape cone is trapped inside the semiconductor and thus likely lost by eventual absorption. Although major efforts have been made to alleviate the light-escape problem, for example, by optimizing the geometrical shape of the LED die[1] and by surface roughening,[2–5] the fundamental problem of the high-refractive-index contrast between semiconductor and air remains unsolved. Encapsulants such as epoxy and silicone reduce the refractive index contrast resulting in a larger light-escape cone, as shown in Fig. 1(a). However, the refractive indices of typical encapsulants are only ~1.5, far below the refractive indices of III-V nitrides and phosphides ($n=2.5–3.5$). The extraction efficiency ratio for light coupled into epoxy to light coupled into air is given by[6]

$$\frac{\eta_{\mathrm{epoxy}}}{\eta_{\mathrm{air}}}=\frac{1-\cos\theta_{c,\mathrm{epoxy}}}{1-\cos\theta_{c,\mathrm{air}}}, \tag{1}$$

where $\theta_{c,\mathrm{epoxy}}$ and $\theta_{c,\mathrm{air}}$ are the critical angles for total internal reflection of the epoxy-semiconductor and air-semiconductor interface, respectively. As the refractive index of the encapsulant increases, the calculated light-extraction efficiency increases rapidly as shown in Fig. 1(b). This represents the clear motivation for developing encapsulants with higher refractive indices than typical epoxies or silicones.

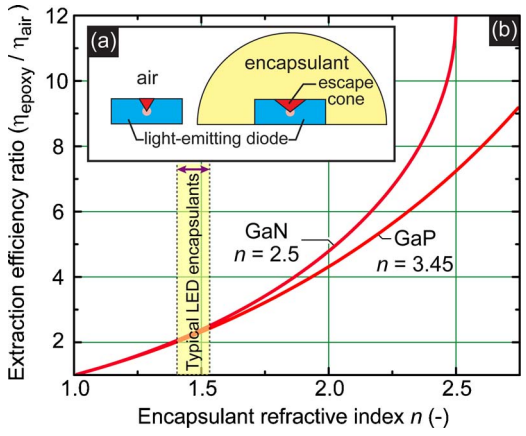

FIG. 1. (Color online) (a) Escape cone of an LED without and with encapsulation. (b) Light-extraction efficiency ratio for GaN and GaP as a function of the encapsulant refractive index.

a)Electronic mail: efschubert@rpi.edu.

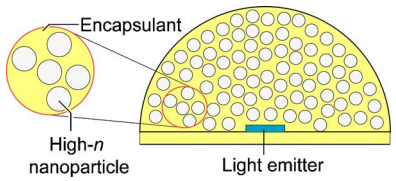

FIG. 2. (Color online) Conceptual drawing of high-n nanoparticle-loaded encapsulant.

High-refractive-index nanoparticles, such as titania (TiO_2, $n_{TiO2}=2.7$), that are dispersed *uniformly* in an encapsulant, as conceptually drawn in Fig. 2, will increase the overall refractive index of the encapsulant.

Consider the phase velocity of an optical wave traveling through a medium, given as

$$v_{ph} = \frac{c}{n}, \tag{2}$$

where c is the speed of light in vacuum and n is the refractive index of the medium. For a given distance, the wave propagation time through TiO_2 will be longer than through neat epoxy due to the higher refractive index of TiO_2. We define the total propagation time by

$$\tau_{tot} = \tau_{TiO2} + \tau_{epoxy}, \tag{3}$$

where τ_{TiO2} and τ_{epoxy} are the propagation times through TiO_2 and epoxy, respectively. A TiO_2-nanoparticle-loaded epoxy medium of volume loading fraction (or volume loading percentage), L, over a distance d, has a total propagation time of

$$\tau_{tot} = \frac{d_{TiO2}}{v_{ph,TiO2}} + \frac{d_{epoxy}}{v_{ph,epoxy}} = \frac{d_{TiO2}n_{TiO2}}{c} + \frac{d_{epoxy}n_{epoxy}}{c}$$
$$= \frac{V_{tot}}{A}\frac{Ln_{TiO2}}{c} + \frac{V_{tot}}{A}\frac{(1-L)n_{epoxy}}{c} = \frac{V_{tot}}{Ac}[Ln_{TiO2} + (1 - L)n_{epoxy}], \tag{4}$$

where V_{tot} is the total volume, A is the cross-sectional area, and we have neglected any dispersion effect. Let us denote the effective refractive index of the TiO_2-loaded epoxy as n_{eff}. We then can write

$$\tau_{tot} = \frac{V_{tot}n_{eff}}{Ac}. \tag{5}$$

Comparison of Eqs. (4) and (5) yields an effective refractive index of

$$n_{eff} = \frac{V_{TiO2}n_{TiO2} + V_{epoxy}n_{epoxy}}{V_{tot}}, \tag{6}$$

where V_{TiO2} and V_{epoxy} are the TiO_2 and epoxy volumes, respectively. The calculated refractive index of the TiO_2-epoxy composite is shown in Fig. 3 as a function of the TiO_2 volume loading fraction L. Inspection of the figure reveals that the refractive index of the TiO_2-epoxy composite increases linearly with the TiO_2 volume loading fraction.

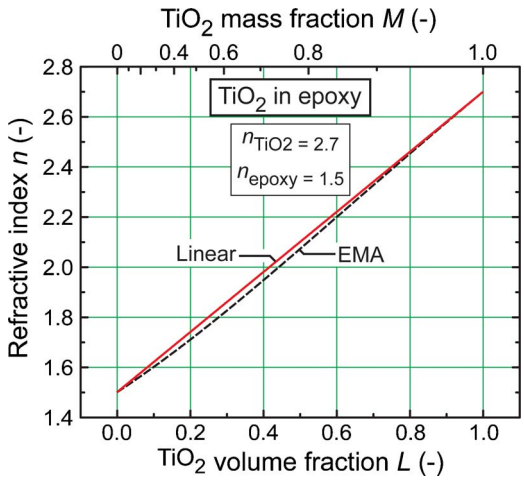

FIG. 3. (Color online) Calculated encapsulant refractive index of TiO_2-nanoparticle-loaded epoxy for linear approximation and effective medium approximation (EMA) in terms of volume loading fraction L and mass loading fraction M.

The effective medium approximation[7] (EMA) is also shown in Fig. 3 with respect to TiO_2 volume loading fraction. Comparison of the two theoretical curves shows that they are very similar.

The volume loading fraction of TiO_2 in epoxy is related to the mass loading fraction by

$$L = \frac{\text{Volume of } TiO_2}{\text{Volume of } TiO_2 + \text{Volume of epoxy}} = \frac{\frac{M}{\rho_{TiO2}}}{\frac{M}{\rho_{TiO2}} + \frac{1-M}{\rho_{epoxy}}}, \tag{7}$$

where M is the TiO_2 mass loading fraction, ρ_{TiO2} is the mass density of TiO_2, and ρ_{epoxy} is the mass density of epoxy. The volume loading fraction has a nonlinear relationship with respect to mass loading fraction, as shown in Fig. 4, due to the density difference of the polymer and TiO_2.

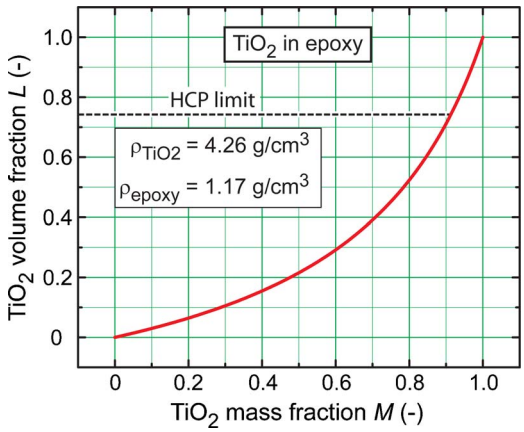

FIG. 4. (Color online) Calculated relation between volume and mass loading fractions for rutile phase TiO_2 in epoxy resin. Hexagonal close-packed (HCP) is the most densely packed crystal lattice structure, similarly, the maximum volume fraction occurs when nanoparticles follow an HCP configuration.

If nanoparticles are in an ordered, latticelike arrangement within a medium, with the nanoparticles having a diameter much less than the wavelength of incident light, then the nanoparticles will not induce optical scattering. In a uniform distribution of nanoparticles, given by the Poisson distribution, Rayleigh scattering will occur due to refractive index fluctuations throughout the medium. Additionally, the high surface-to-volume ratios at the nanoscale often favor attractive forces between nanoparticles, which result in their agglomeration. The tendency of nanoparticles to agglomerate will result in excess optical scattering, i.e., scattering will be larger than Rayleigh scattering. Therefore, to realize high-n nanoparticle-loaded encapsulants without scattering and absorption losses, uniform dispersion and stabilization of nanoparticles are needed.

In the present work, we demonstrate an increase in refractive index of TiO_2-nanoparticle-loaded epoxy by uniform dispersion of surfactant-coated TiO_2 nanoparticles in epoxy. The Rayleigh scattering of TiO_2-nanoparticle-loaded epoxy is highly dependent upon nanoparticle radius and volume loading fraction. A graded-refractive-index-encapsulation concept is proposed to reduce optical losses by scattering and Fresnel reflections. Furthermore, three-dimensional ray-tracing simulations are performed to investigate how optical scattering by nanoparticles influences the light-extraction efficiency. We show that scattering by nanoparticles in encapsulants can strongly improve light extraction when the scattering coefficient k_s is optimized.

II. EXPERIMENT AND RESULTS

TiO_2 commercial nanoparticles from Nanophase Technologies Corporation of average diameter of 40 nm have a surface area of 35 m^2/g, illustrating the enormous importance of surface effects. The TiO_2 nanoparticles are produced by a vapor-phase method, in which electrical arc energy is applied to solid titanium to generate titanium vapors at a high temperature. Then, oxygen is added to the vapor, cooled at a controlled rate so that the titanium atoms react with oxygen and condense to form TiO_2 nanoparticles. X-ray diffraction analysis of the TiO_2 nanoparticles shows that the dominant crystal structure is the rutile phase. TiO_2 has a refractive index of 2.7 at 500 nm. Usually, as-received TiO_2 nanoparticles contain ~1 wt % of molecular water and surface hydroxyls. Figure 5(a) shows an optical micrograph of the as-received TiO_2 nanoparticles. Many of the TiO_2 nanoparticles stick together to form weak agglomerates possibly due to adsorbed molecular water and hydroxyls on the surface of the nanoparticles.[9] A cleaning/drying process is carried out at 125 °C in an N_2 ambient-pressure glove box for 24 h to dry the nanoparticle surfaces. In an effort to prevent the reabsorption of H_2O and other containments after the drying step, the particles are immediately mixed in toluene and magnetically stirred. Then, appropriate amounts of surfactant A or B (Ref. 8) are mixed into the solution. The surfactants adsorb onto the nanoparticle surface and modify inter-particle forces thereby enhancing particle dispersibility. To coat the nanoparticles with the surfactants effectively, a reflux system is used for 48 h. In the refluxing process, a solution is heated near its boiling point; the vapor produced rises and condenses back to the solution after coming in contact with a water-cooled surface. The purpose of refluxing is to thoroughly mix the surfactant with the nanoparticles to produce a solution of nonagglomerated nanoparticles. The resulting solution is placed in a centrifuge for removal of toluene. The nanoparticles are subsequently washed with new toluene to remove additional contaminants and recentrifuged. The resultant surface-modified TiO_2 nanoparticles are dried at 125 °C in an N_2 ambient-pressure glove box for 24 h. After drying, the surface-modified TiO_2 nanoparticles are mixed into epoxy via a planetary mixer. For curing preparation, a cationic photoinitiator is added into the solution. The nanoparticle loaded epoxy is spin coated on a silicon substrate and exposed to ultraviolet radiation from a xenon lamp for 90 s to complete curing.

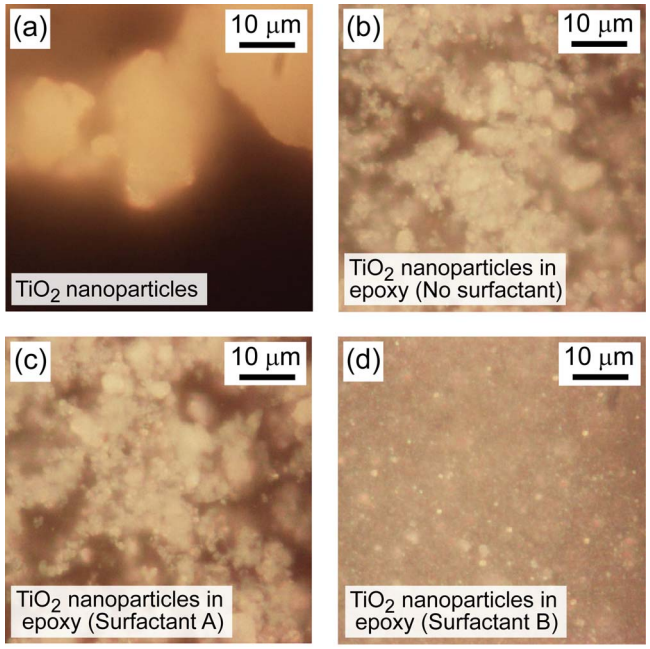

FIG. 5. (Color online) Optical micrographs of TiO_2 nanoparticles (a) as received, (b) dispersed in epoxy without surface treatment, (c) with surfactant A, and (d) with surfactant B.

Figure 5(b) shows an optical micrograph of TiO_2 nanoparticles dispersed in epoxy without surface modification, and, as a consequence, significant agglomeration of TiO_2 nanoparticles is observed. Figures 5(c) and 5(d) show optical micrographs of surface-modified TiO_2 nanoparticles dispersed in epoxy with surfactants A and B, respectively. Comparison of the micrographs demonstrates that the chemistry of the surfactant directly affects the dispersibility of the nanoparticles in polymeric materials. Significant agglomeration of the nanoparticles is still observed with the nanoparticles coated by surfactant A. However, when the surface of the TiO_2 nanoparticles is modified by using the proper surfactant, surfactant B, particle dispersibility is drastically enhanced, as shown in Fig. 5(d).

The spectral reflectivity of TiO_2-loaded epoxy and unloaded (neat) epoxy spin coated on silicon are measured, as shown in Figs. 6(a) and 6(b), respectively. The reflectivity curves contain periodic oscillations, whose simulation indi-

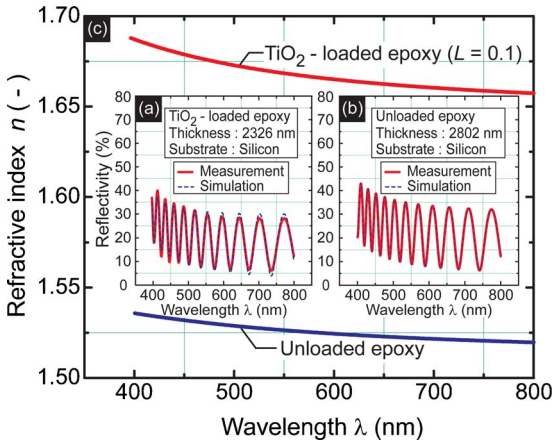

FIG. 6. (Color online) Reflectivity vs wavelength for (a) TiO_2-loaded epoxy (L=0.1) and (b) unloaded epoxy with corresponding plots of (c) refractive indices versus wavelength based on the Cauchy model.

cates film thicknesses of 2.33 and 2.80 μm for TiO_2-loaded epoxy and unloaded epoxy, respectively. The thickness values are also measured by ellipsometry and cross-sectional scanning electron microscopy (SEM) and these measurements agree with the thicknesses of the spectral reflectivity simulation. Based on the wavelength dependent reflectivity curves, the refractive index of TiO_2-loaded epoxy and unloaded epoxy is evaluated using the Cauchy model, which expresses the refractive index as

$$n(\lambda) = A_n + \frac{B_n}{\lambda^2} + \frac{C_n}{\lambda^4}, \tag{8}$$

where A_n, B_n, and C_n are constants. Inspection of Fig. 6(c) indicates a clear increase of refractive index for the TiO_2-loaded encapsulant with loading factor L=0.1 (n =1.67 at λ=500 nm) compared to unloaded epoxy (n=1.53 at λ=500 nm). The refractive index value of the TiO_2-loaded encapsulant with loading factor L=0.1 follows the trend shown in Fig. 3. The overall reflectivity values of the TiO_2-nanoparticle-loaded encapsulant are less compared to unloaded epoxy signifying a refractive index enhancement due to the reduction in reflectance at the Si-epoxy interface for the high-refractive-index medium (the reflectance from the epoxy-air interface is less significant at these encapsulant refractive index values).

III. DISCUSSION

A. Scattering by nanoparticles

The refractive index variation inside high-n nanoparticle-loaded encapsulants results in optical scattering by nanoparticles. If the particle size is much less that the wavelength of light (e.g., one-tenth of the wavelength), Rayleigh scattering is the dominant scattering mechanism. The Rayleigh scattering cross section of a nanoparticle inside a polymer host is given by[10]

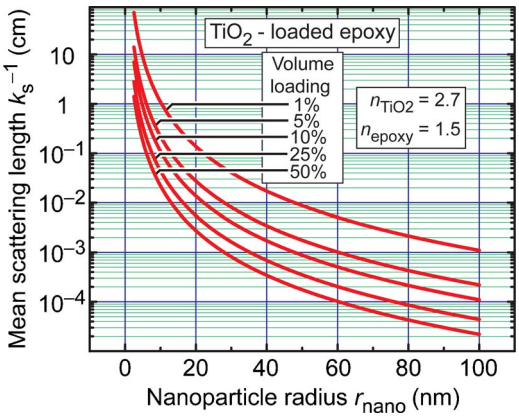

FIG. 7. (Color online) Mean distance between scattering events of TiO_2 nanoparticles in epoxy as a function of nanoparticle radius for volume loading fractions of 0.01, 0.05, 0.10, 0.25, and 0.5.

$$C_{\text{scat}} = \frac{8\pi r_{\text{nano}}^6}{3} k^4 \left| \frac{n_{\text{nano}}^2 - n_{\text{host}}^2}{n_{\text{nano}}^2 + 2n_{\text{host}}^2} \right|^2, \tag{9}$$

where r_{nano} is the radius of the spherical nanoparticle, k is the wave number ($2\pi/\lambda$), and n_{nano} and n_{host} are the refractive indices of the nanoparticle and polymer host, respectively. Rearranging terms in Eq. (9) yields

$$C_{\text{scat}} = \frac{2\pi^5}{3} n_{\text{host}}^4 \left(\frac{n_{\text{nano}}^2 - n_{\text{host}}^2}{n_{\text{nano}}^2 + 2n_{\text{host}}^2} \right)^2 \frac{(2r_{\text{nano}})^6}{\lambda_0^4}. \tag{10}$$

The scattering cross section is related to the scattering coefficient k_s by

$$k_s = NC_{\text{scat}}, \tag{11}$$

where N is the concentration of scattering centers (nanoparticles per unit volume), which is equal to L/V_{nano}, where L is volume loading fraction. Therefore, the Rayleigh scattering coefficient of a nanoparticle-loaded polymer is

$$k_s = \frac{2\pi^5}{3} \left(\frac{n_{\text{nano}}^2 - n_{\text{host}}^2}{n_{\text{nano}}^2 + 2n_{\text{host}}^2} \right)^2 \frac{(2r_{\text{nano}})^6}{(\lambda_0/n_{\text{host}})^4} \frac{L}{(4/3)\pi r_{\text{nano}}^3}. \tag{12}$$

The inverse of the scattering coefficient, $1/k_s$, which is the mean distance between scattering events, is highly dependent upon nanoparticle radius and volume loading fraction. Figure 7 shows the calculated mean scattering length of TiO_2-loaded epoxy with various nanoparticle radii at specified loadings assuming n_{nano}=2.7, n_{host}=1.5, at λ=500 nm. For a nanoparticle of radius of 20 nm and a volume loading fraction of 0.5 in epoxy (n_{host}=1.5), the mean scattering length is k_s^{-1}=27 μm. This calculation illustrates that, in this case, the *specular transparency* (transparency of a medium with little scattering) can be obtained only for films with thickness up to 27 μm.

B. Graded-index encapsulation

Non graded high-n nanoparticle-loaded encapsulants will produce Fresnel-reflection losses at the abrupt encapsulant-air interface. Nanoparticle-loaded encapsulants that consist of multiple encapsulant layers with gradually decreasing refractive-index values, whose layer thicknesses are less than the mean scattering length to maintain specular

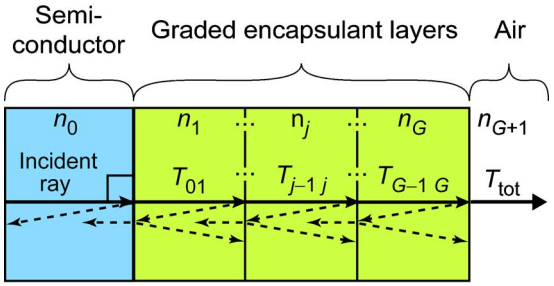

FIG. 8. (Color online) Structure for calculating total transmittance from a semiconductor of refractive index n_0 through a graded-refractive-index encapsulant with a number of layers G to air.

or quasispecular transparency, will minimize Fresnel reflection and scattering losses while maximizing transmittance. The reflection at normal incidence can be expressed in terms of the Fresnel transmission coefficient for two media as

$$T_f = \frac{4n_1 n_2}{(n_1 + n_2)^2}, \tag{13}$$

where n_1 and n_2 are the refractive index values of media 1 and 2, respectively. For a graded encapsulant, multiple reflection and transmission events at each interface will contribute to the overall transmittance and reflectance, as shown in Fig. 8. Accounting for multiple reflections within a layer bounded by refractive index contrasts, we analytically find that the total transmittance for a graded encapsulant of G layers can be expressed as[11,12]

$$T_{\text{tot}} = 4\frac{n_0 n_1}{(n_0 + n_1)^2}\prod_{j=2}^{G+1}\frac{4\cdot\dfrac{n_{j-1}n_j}{(n_{j-1}+n_j)^2}}{\left(1-\dfrac{(n_{j-1}-n_{j-2})^2}{(n_{j-1}+n_{j-2})^2}\dfrac{(n_{j-1}-n_j)^2}{(n_{j-1}+n_j)^2}\right)}, \tag{14}$$

where n_0 and n_{G+1} are the semiconductor and air refractive index values, respectively, and $n_1, n_2, \ldots, n_G$ represent the graded-index encapsulant layers following n_0.

The refractive index value of each layer should be optimized to yield maximum transmittance based on Eq. (14). We find that the optimal refractive index producing maximum transmittance for G layers is given by[11,12]

$$n_m \approx (n_0)^{m/(G+1)}, \tag{15}$$

where $m = 1, 2, \ldots, G$ is the first, second, and Gth, layer placed on top of the semiconductor.

Assuming normally incident light for a graded-index encapsulant, as shown in Fig. 9(a), Eqs. (13) and (14) can be used to calculate the GaN and GaP transmittance values for encapsulant layers that are so thick that thin-film interference effects can be neglected. Figure 9(b) shows the calculated transmittance from GaN ($n=2.5$) and GaP ($n=3.45$) to air ($n=1.0$) while varying the number of optimized encapsulant layers based on Eqs. (14) and (15). Optical transmittance is significantly enhanced as the number of layers increases due to the strong reduction of Fresnel reflection.

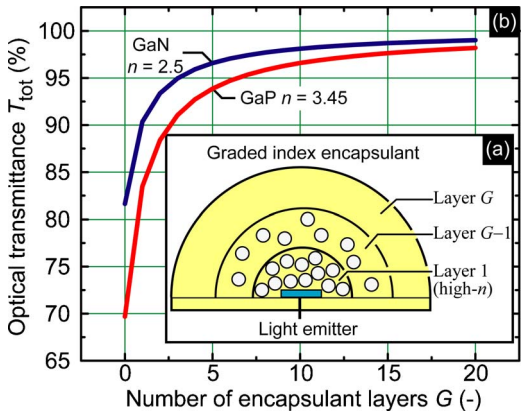

FIG. 9. (Color online) (a) Calculated normal incidence optical transmittance for GaN and GaP for (b) a step-graded-index encapsulant.

C. Optimum scattering for light extraction

Three-dimensional ray-tracing simulations are performed in order to investigate the effect of optical scattering by nanoparticles in an encapsulant on light-extraction efficiency. A lambertian surface emitter located inside a lightly absorbing cubic encapsulant of volume $(5\text{ mm})^3$ is shown in Fig. 10. Optically trapped modes in the encapsulant are generated from light obliquely incident at the encapsulant-air refractive-index boundary due to total internal reflection. For weak scattering, the deterministic trapped modes are unable to escape into free space and are ultimately absorbed by the encapsulant. For strongly scattering nanoparticle-loaded encapsulants, the optical scattering length, k_s^{-1}, is short, but the light rays' optical path length is long. The long optical path length eventually exceeds the photon absorption length, α^{-1}, resulting in photon absorption by the encapsulant, thus decreasing light-extraction efficiency. The light rays that escape the cubic encapsulant are captured by a far-field receiver, which is used to assess the light-extraction efficiency value of the lambertian surface emitter. An optimized amount of scattering is beneficial, as shown in Fig. 10, which indicates that the enhancement of light-extraction efficiency is greater than 50% for an optimized scattering coefficient k_s. An encapsulant with an optimized k_s will enhance light-extraction efficiency by optically scattering the deterministic trapped

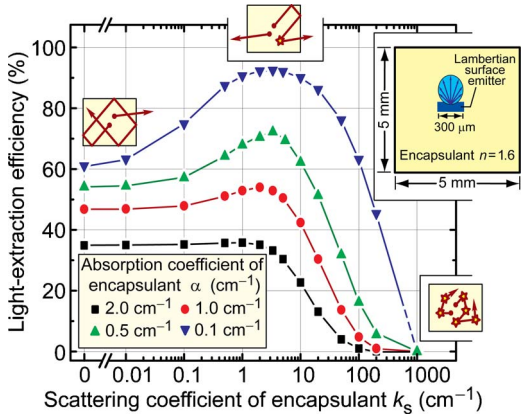

FIG. 10. (Color online) Three-dimensional ray-tracing simulation of light-extraction efficiency vs scattering coefficient for a lambertian surface emitter inside an encapsulant of $(5\text{ mm})^3$ for different absorption coefficients.

modes of light into free space. Therefore, remote phosphor-based LEDs (Ref. 13) that contain whispering gallery modes[14] will benefit greatly from an encapsulant with an optimized scattering coefficient k_s.

IV. CONCLUSIONS

TiO_2-nanoparticle-loaded encapsulants for LEDs are fabricated. As-received TiO_2 nanoparticles with average diameter of 40 nm are dried, mixed with a solvent, refluxed, centrifuged, and mixed with epoxy to produce surfactant-coated nanoparticles. A drastic reduction of TiO_2 agglomeration in epoxy is observed for surfactant-coated TiO_2 nanoparticles. The refractive index of the TiO_2-nanoparticle-loaded epoxy film is $n=1.67$ at $d=500$ nm, much higher than that of conventional unloaded epoxy, $n=1.53$ at $\lambda=500$ nm. Theoretical calculations indicate that the optical scattering in nanoparticle-loaded epoxy is highly dependent upon the radius and volume loading fraction of the dispersed nanoparticles. For the reduction of optical losses by scattering and Fresnel reflection by nanoparticle-loaded encapsulants, we propose a graded-index multilayer encapsulation with layer thicknesses less than the mean optical scattering length. In addition, ray-tracing simulations reveal that optical scattering in encapsulants does not necessarily reduce light-extraction efficiency; rather, it is shown that an enhancement greater than 50% can occur for encapsulants with an optimized scattering coefficient.

ACKNOWLEDGMENTS

We gratefully thank the National Science Foundation, Troy Research Corporation, Department of Energy, Crystal IS Corporation, Samsung Advanced Institute of Technology, Sandia National Laboratories, and New York State for support. This work was supported in part by the Nanoscale Science and Engineering Initiative of the National Science Foundation under NSF Award No. DMR-0117792. The authors would like to gratefully acknowledge ray-tracing contributions from Hong Luo to this work.

[1] M. R. Krames, M. Ochiai-Holcomb, G. E. Höfler, C. Carter-Coman, E. I. Chen, I.-H. Tan, P. Grillot, N. F. Gardner, H. C. Chui, J.-W. Huang, S. A. Stockman, F. A. Kish, M. G. Craford, T. S. Tan, C. P. Kocot, M. Hueschen, J. Posselt, B. Loh, G. Sasser, and D. Collins, Appl. Phys. Lett. **75**, 2365 (1999).
[2] B. van Ginneken, M. Stavridi, and J. J. Koenderink, Appl. Opt. **37**, 130 (1998).
[3] T. R. Thomas, *Rough Surfaces* (Imperial College Press, London, 1999).
[4] T. Fujii, Y. Gao, R. Sharma, E. L. Hu, S. P. DenBaars, and S. Nakamura, Appl. Phys. Lett. **84**, 855 (2004).
[5] Y. Xi, X. Li, J. K. Kim, F. Mont, Th. Gessmann, H. Luo, and E. F. Schubert, J. Vac. Sci. Technol. A **24**, 1627 (2006).
[6] E. F. Schubert, *Light Emitting Diodes* (Cambridge University Press, Cambridge, U. K., 2003).
[7] J. K. Kim, Th. Gessmann, E. F. Schubert, J.-Q. Xi, H. Luo, J. Cho, C. Sone, and Y. Park, Appl. Phys. Lett. **88**, 013501 (2006).
[8] The chemical compositions of surfactant A and surfactant B are trade secrets of Troy Research Corporation and cannot be publicly disclosed.
[9] F. W. Mont, H. Luo, M. F. Schubert, J. K. Kim, E. F. Schubert, and R. W. Siegel, Mater. Res. Soc. Symp. Proc. **955E**, I13–02 (2006).
[10] H. C. van de Hulst, *Light Scattering by Small Particles* (Dover, New York, 1981).
[11] F. W. Mont, J. K. Kim, M. F. Schubert, H. Luo, E. F. Schubert, and R. W. Siegel, Proc. SPIE **6486**, 64861C (2007).
[12] F. W. Mont, M.S. Thesis, Rensselaer Polytechnic Institute, 2006.
[13] J. K. Kim, H. Luo, E. F. Schubert, J. Cho, C. Sone, and Y. Park, Jpn. J. Appl. Phys., Part 2 **44**, L649 (2005).
[14] H. Luo, J. K. Kim, Y. A. Xi, E. F. Schubert, J. Cho, C. Sone, and Y. Park, Appl. Phys. Lett. **89**, 041125 (2006).